

# Complete and generalized synchronization of chaos and hyperchaos in a coupled first-order time-delayed system

Tanmoy Banerjee · Debabrata Biswas ·  
B.C. Sarkar

Received: 25 September 2012 / Accepted: 24 October 2012 / Published online: 8 November 2012  
© Springer Science+Business Media Dordrecht 2012

**Abstract** This paper explores the synchronization scenario of coupled chaotic and hyperchaotic time delay systems that are coupled through linear, dissipative and unidirectional coupling. For the present study, we choose a prototype first-order nonlinear time delay system, which is recently reported in Banerjee et al. (Nonlinear. Dyn., doi:10.1007/s11071-012-0490-3, 2012); the system shows well-characterized chaotic and hyperchaotic oscillations even for a small time delay, and also, experimental implementation of the system is easy. We show that, keeping all the system design parameters the same for the two systems, if the time delays associated with the two systems are equal, then complete synchronization occurs beyond a threshold coupling strength. On the contrary, above a certain coupling strength, generalized synchronization between two identical coupled systems occurs for the unequal time delays. We derive an estimate of the coupling strength and sufficient stability conditions for all the synchronization processes using Krasovskii–Lyapunov theory. We simulate the coupled system numerically to support the analytical results. Also, we implement the coupled system in an electronic circuit to verify all the synchronization phenomena. It

is shown that the experimental results agree well with our analytical and numerical results.

**Keywords** Delay dynamical system · Chaos synchronization · Hyperchaos · Time delay electronic circuit

## 1 Introduction

For the last two decades synchronization of chaos has been an active area of research in various fields, including physics, biology, mathematics, engineering, etc. In a seminal paper Pecora and Carrol [2] have first shown that two chaotic trajectories having different initial conditions can be synchronized. Since then researchers around the world have been actively engaged to explore different possible synchronization scenario of the chaotic systems; the following variety of synchronization schemes have been observed and identified: Complete synchronization [2], Generalized synchronization [3–5], Phase synchronization [6], Lag synchronization [7, 8], Anticipatory synchronization [9], Impulsive synchronization [10, 11], etc. Two excellent review papers [12, 13] describe the state of the present status of synchronization of chaos.

In the initial years, emphasis has been on the synchronization of low dimensional chaotic systems, i.e., chaotic systems having a single positive Lyapunov exponent (LE). Later on, synchronization of higher dimensional chaos (i.e. hyperchaos) [14], and chaotic

---

T. Banerjee (✉) · D. Biswas · B.C. Sarkar  
Department of Physics, The University of Burdwan,  
Burdwan 713104, West Bengal, India  
e-mail: tanbanrs@yahoo.co.in

T. Banerjee  
e-mail: tanban.buphys@gmail.com

oscillators in a network [15] have also been extensively studied. In the former category, the most important system is nonlinear delay dynamical system (DDS), which is modeled by delay differential equations (DDE). DDS is an infinite dimensional system having a large number of positive Lyapunov exponents. DDEs have been successfully used to model various natural phenomena; examples include: blood production in patients with leukemia (Mackey–Glass model) [16], dynamics of optical systems (e.g. Ikeda system) [17, 18], population dynamics [19], physiological models [20], the El Niño/southern oscillation (ENSO) [21], neural networks [22], control systems [23–25], etc. Further, coupled time-delayed systems exhibit interesting phenomena like amplitude death [26], multistability, etc. that cannot be anticipated by a low dimensional system. Thus studies on the coupled delay dynamical systems and identify the conditions of their synchronization regime have been a potential research problem. Pyragas [27] first shown that time-delayed chaotic systems can be properly coupled to make them synchronous. Later, depending on the coupling delay and feedback delay many synchronization phenomena have been reported [28–31].

Apart from the academic interest, synchronization of chaotic and hyperchaotic delay dynamical systems offers a great opportunity to the researchers to harness the richness of hyperchaos, having multiple positive Lyapunov exponents (LEs) [32]. It has already been established that communication with a low dimensional chaos (having a single positive LE) is not fully secure because an eavesdropper can reconstruct the chaotic attractor and retrieve the hidden message [33]. Therefore, synchronization of hyperchaotic systems has been proposed as an alternative method for improving the security in the communication schemes [14]. As a simple time-delay system with suitable nonlinearity can produce a hyperchaotic signal with multiple positive LEs, they have been identified as good candidates for secure communication system [34].

In order to realize a chaos-based communication system the first step is to design *simple* and *well characterized* time-delay systems that can produce chaos and hyperchaos. Nonlinear time-delayed systems that can be implemented with off-the-shelf electronic circuits are of particular interest due to their application potentiality; that is why, many electronic circuits and systems have been reported in the literature. Most of the circuits reported in literature used piece-wise-linear (PWL) nonlinearity for the ease of circuit design

and analysis [35–40]. But an exact analysis and circuit implementation of those PWL circuits are not possible. In Ref. [1], we proposed a time-delayed chaotic and hyperchaotic system having a *closed form mathematical function* of the nonlinearity. With detailed bifurcation analysis and numerical simulations we established that the system is a potential chaos and hyperchaos generator even with a *small* or *moderate* time delay. Also the system was experimentally designed with off-the-shelf electronic circuits, and chaotic and hyperchaotic attractors were observed experimentally.

In this paper we study the synchronization of two unidirectionally coupled chaotic (hyperchaotic) nonlinear time-delay systems that are recently proposed in [1]. The time-delayed systems are coupled through a linear dissipative coupling. It is shown that if we consider two identical systems with the same system delays, then complete synchronization occurs beyond a threshold coupling strength. On the other hand, if we consider two identical systems with unequal time delays, generalized synchronization occurs. Stability conditions of all the synchronization processes are analytically obtained using Krasovskii–Lyapunov theory. Numerical simulations are carried out to observe different synchronization scenario. It is shown that numerical results corroborate the analytical findings. Finally, we set up an electronic circuit experiment to experimentally verify all the synchronization scenario described in this paper. We show that experimental results agree well with the analytical and numerical results.

The paper is organized in the following manner: the next section describes the time-delayed system [1] and a summary of its dynamical behavior. Section 2 describes the coupled system along with the proper coupling schemes. Stability analysis using Krasovskii–Lyapunov theory is given in Sect. 4. Numerical simulations of different synchronization schemes are reported in Sect. 5. Section 6 reports the circuit implementation of the coupled system. Experimental results are described in Sect. 7. Finally, Sect. 8 concludes the outcome of the whole study.

## 2 System description and dynamics of the uncoupled system

In this section we describe the time-delayed system proposed in Ref. [1], and also briefly discuss its important dynamical features. Reference [1] proposed

the following first-order, nonlinear, retarded type delay differential equation with a single constant delay:

$$\dot{x} = -ax(t) - bf(x_\tau), \tag{1}$$

where  $a$  and  $b$  are system parameters,  $a > 0$  and  $b > 0$ . Also,  $x_\tau \equiv x(t - \tau)$ , where  $\tau \in \mathbb{R}^+$  is a constant time delay. Nonlinearity  $f(x_\tau)$  is defined by the following closed form mathematical function:

$$f(x_\tau) = -0.5n(|x_\tau| + x_\tau) + m \tanh(lx_\tau), \tag{2}$$

where  $n$ ,  $m$ , and  $l$  are all positive system parameters. Figure 1 shows the nature of the nonlinearity of  $f(x_\tau)$  for different values of  $n$ ,  $m$  and  $l$ . There exist a large number of choices of  $n$ ,  $m$  and  $l$  that can produce this particular nature of the nonlinearity. The nonlinearity shows a single hump in the first quadrant, but unlike the nonlinearity of Mackey–Glass (MG) system [16], it does not asymptotically vanish.

The detailed stability and bifurcation analysis was reported in [1]; there we have proved the existence of chaos and hyperchaos through the presence of strange attractor along with positive Lyapunov exponent and higher values ( $> 3$ ) of Kaplan–York dimension [41]. The following parameter values have been used in [1]:  $a = 1$ ,  $n = 1.15$ ,  $m = 0.97$ ,  $l = 2.19$ . It has been shown that, keeping  $b$  fixed, if one varies  $\tau$ , the system shows a period doubling route to chaos and hyperchaos [1]. For example, for  $b = 1.7$ , at  $\tau = 0.805$ , the fixed point loses its stability through Hopf bifurcation and a stable limit cycle appears; chaos and hyperchaos are observed at  $\tau \approx 3.1$  and  $\tau \approx 3.60$ , respectively. Further, keeping  $\tau$  fixed, if we vary  $b$  then also chaos and hyperchaos occur; e.g., at  $\tau = 4$ , chaos occurs for  $b \geq 1.52$  and hyperchaos occurs for  $b \geq 1.75$ . Figure 2 shows the chaotic and hyperchaotic attractors for different time delays (with  $b = 1.7$ ). Figure 3 explores the dynamics of the system in the whole  $b$ – $\tau$  parameter space. It is noteworthy that for a proper choice of  $b$ , the system shows chaos and hyperchaos even for a small time delay; e.g. for  $b = 2.25$  one has chaos for  $\tau \approx 1.85$ . This makes the circuit implementation of the system is easier and also makes it superior for the possible applications in communication system.

### 3 Coupled time-delayed system

Let us consider two chaotic systems given by (1) coupled through a linear, dissipative, unidirectional cou-

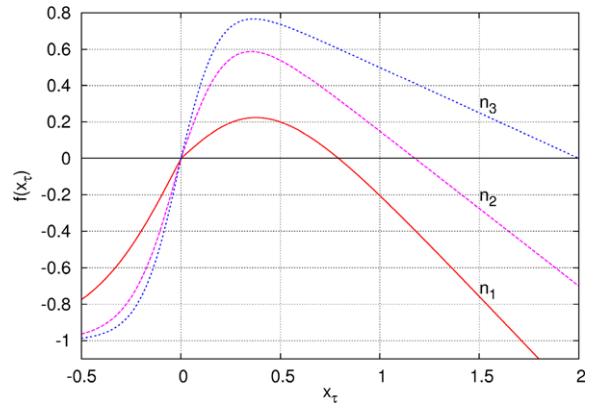


**Fig. 1** Nonlinearity with the function  $f(x_\tau) = -n0.5(|x_\tau| + x_\tau) + m \tanh(lx_\tau)$  with  $n_1$ :  $n = 1.15$ ,  $m = 0.97$ ,  $l = 2.19$ ;  $n_2$ :  $n = 0.8$ ,  $m = 1$ ,  $l = 4$ ,  $n_3$ :  $n = 1.5$ ,  $m = 1$ ,  $l = 6$

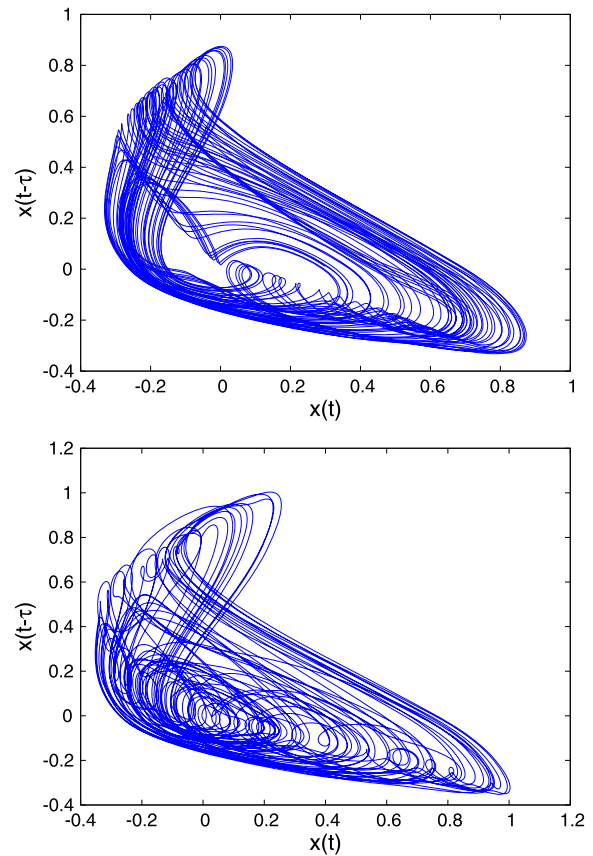


**Fig. 2** Phase plane plot in  $x$ – $x(t - \tau)$  space for different  $\tau$ : (upper panel)  $\tau = 3.17$  (chaos), (lower panel)  $\tau = 4.78$  (hyperchaos) (other parameters are:  $b = 1.7$ ,  $a = 1$ ,  $n = 1.15$ ,  $m = 0.97$ ,  $l = 2.19$ )

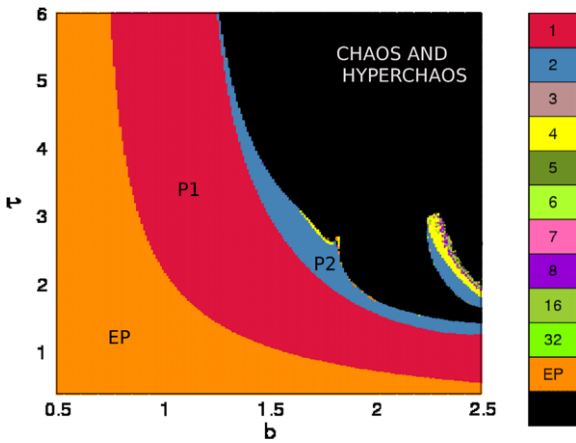


**Fig. 3** Two parameter bifurcation diagram of  $x$  in the  $b - \tau$  space. *Color-box* represents the period of oscillations; *EP* stands for equilibrium point. It is noteworthy that for a proper choice of  $b$  one has chaos and hyperchaos even for  $\tau < 2$  (other parameters are:  $a = 1, n = 1.15, m = 0.97, l = 2.19$ ) (Color figure online)

pling. The mathematical model of the coupled system is given by

$$\dot{x} = -ax(t) - b_1 f(x_{\tau_1}), \tag{3a}$$

$$\dot{y} = -ay(t) - b_2 f(y_{\tau_2}) + K(x - y). \tag{3b}$$

where  $a > 0$  is a constant,  $b_1$  and  $b_2$  are called the feedback rates for the two systems.  $\tau_1$  and  $\tau_2$  are the system delays.  $K$  is the coupling rate that determines the strength of the coupling.  $x$  is designated as the *driver* and  $y$  is the *response* system.

### 4 Stability analysis of the coupled system

In this section we will derive the asymptotic stability condition of synchronization and also find an estimate of the coupling rate beyond which synchronization occurs. If all other system parameters are same for the two systems, two types of synchronization scenario are possible, namely, the complete synchronization (for  $\tau_1 = \tau_2$ ) and the generalized synchronization (for,  $\tau_1 \neq \tau_2$ ) [29]. In the following subsections we investigate the stability for each synchronization process.

#### 4.1 Complete synchronization

For the complete synchronization we must have  $\tau_1 = \tau_2$ , such that the synchronization manifold becomes  $x = y$ . We introduce the error function defined

as  $\Delta = (x - y)$ . The time evolution of the error yields the error dynamics of systems (3a) and (3b) as

$$\begin{aligned} \frac{d\Delta}{dt} = & -(a + K)\Delta + (-b_1 + b_2)f(x_{\tau_1}) \\ & - b_2 f'(x_{\tau_1})\Delta_{\tau_1}. \end{aligned} \tag{4}$$

This is an inhomogeneous equation and hence difficult to analyze. To make it homogeneous we impose the constraint

$$b_1 = b_2. \tag{5}$$

Obviously, we have to obey this constraint for complete synchronization in order to avoid any parameter mismatch. The error dynamics thus becomes

$$\frac{d\Delta}{dt} = -(a + K)\Delta - b_2 f'(x_{\tau_1})\Delta_{\tau_1}. \tag{6}$$

The synchronization threshold of the coupled system is analyzed with the help of Krasovskii–Lyapunov theory [42]. According to this theory, driver and response (3a), (3b) systems are said to be synchronized if the origin of (6) is stable. To estimate the sufficient condition of stability we introduce a positive definite functional  $V(t)$ :

$$V(t) = \frac{1}{2}\Delta^2 + \mu \int_{-\tau_1}^0 \Delta^2(t + \varphi) d\varphi. \tag{7}$$

Here  $\mu > 0$  is an arbitrary positive parameter. The origin of (6) is said to be stable if the time derivative of  $V(t)$  is negative one. We have

$$\begin{aligned} \frac{dV}{dt} = & -(a + K)\Delta^2 - b_2 f'(x - \tau_1)\Delta\Delta_{\tau_1} \\ & + \mu\Delta^2 - \mu\Delta_{\tau_1}^2. \end{aligned} \tag{8}$$

The condition of negativity of the quantity  $dV/dt$ , for all values of  $\Delta$  and  $\Delta_{\tau_1}$ , reads

$$a + K > \frac{b_2^2 f'^2(x_{\tau_1})}{4\mu} + \mu = \Phi(\mu). \tag{9}$$

Here  $\Phi(\mu)$  is a function of  $\mu$ . At the minimum value of this function we get  $\mu = |b_2 f'(x_{\tau_1})|/2$ , and  $\Phi_{\min} = |b_2 f'(x_{\tau_1})|$ . With these, (9) becomes

$$a + K > |b_2 f'(x_{\tau_1})|. \tag{10}$$

This is the sufficient condition for asymptotic stability of complete synchronization manifold  $x = y$  of (3a), (3b). Here we have to calculate  $f'(x_{\tau_1})$  from (2).

## 4.2 Generalized synchronization

The generalized synchronization arises for the parameter mismatch case; when the system delays are not equal to each other, i.e.,  $\tau_1 \neq \tau_2$ , then generalized synchronization will occur even if the other parameters are same in the two systems. In the case of generalized synchronization, the state of the response ( $y(t)$ ) is related to the driver ( $x(t)$ ) by some functional relationship, i.e.,  $y(t) = g(x(t))$ . To detect generalized synchronization, we use the auxiliary system method of generalized synchronization [4]. According to this method, a new auxiliary dynamical system  $z(t)$  is defined, which is driven by the driver ( $x$ ) with a coupling rate ( $K$ ) equal to that of the response system ( $y(t)$ ). The complete synchronization between  $y(t)$  and  $z(t)$  is the confirmation of generalized synchronization between  $x(t)$  and  $y(t)$ . This method actually enables us to find the stability condition locally for the generalized synchronization. Thus, we investigate for the complete synchronization between the following systems:

$$\dot{y} = -ay(t) - b_2 f(y_{\tau_2}) + K(x - y), \quad (11a)$$

$$\dot{z} = -az(t) - b_2 f(z_{\tau_2}) + K(x - z). \quad (11b)$$

The stability condition of complete synchronization between these two systems are obtained by a similar process as discussed in the previous subsection 4.1, which is

$$a + K > |b_2 f'(y_{\tau_2})|. \quad (12)$$

This, in turn, gives the condition for generalized synchronization between  $x(t)$  and  $y(t)$ . Note that, this is the sufficient condition, which is stable locally for the generalized synchronization.

## 5 Numerical simulation

The system equation (3a), (3b) has been simulated numerically using the Runge–Kutta algorithm with step size  $h = 0.01$ . The following initial functions have been used for all the numerical simulations: for the driver  $\phi_D(t) = 1$ , for the response  $\phi_R(t) = 0.9$ , and for the auxiliary system  $\phi_A(t) = 0.85$ . Also, the following system design parameters are chosen throughout the paper:  $a = 1$ ,  $n = 1.15$ ,  $m = 0.97$ ,  $l = 2.19$  [1]. While presenting the real time and phase plane

diagrams, a large number of iterations have been excluded to allow the system to settle to the steady state.

### 5.1 Complete synchronization: $\tau_1 = \tau_2$

At first we take equal time delays for both the systems i.e.,  $\tau_1 = \tau_2 = 4$ . For the systems to be in the chaotic region we take  $b_1 = b_2 = 1.65$ . For our present choice of parameters, we find from (2) that the maximum value of  $f'(x_{\tau_1})$  is equal to 2.114. Thus from our analytical stability condition (10), the sufficient condition of complete synchronization is  $K \geq 2.488$  (remembering  $a = 1$ ). To ensure complete synchronization, we choose the value of coupling rate higher than that; here we take  $K = 3$ . Figure 4 shows the real time traces of the driver ( $x(t)$ ) and response ( $y(t)$ ), from which we conclude that the driver and response match exactly and thus indicate complete synchronization. This statement is well supported by the phase plane plot in the  $x(t)$ – $y(t)$  plane that shows a straight line making  $45^\circ$  angle with the  $x$ -axis.

Similarly, for the hyperchaotic case we take  $b_1 = b_2 = 2.1$ ; thus (10) suggests that the sufficient condition of complete synchronization is  $K \geq 3.44$ ; for the numerical simulations we chose  $K = 3.5$ . Figure 5 shows the real time traces of the driver ( $x(t)$ ) and response ( $y(t)$ ) and its phase plane representation, which shows an exact similarity between the driver and response indicating complete synchronization.

### 5.2 Generalized synchronization: $\tau_1 \neq \tau_2$

Next, we consider unequal time delays in two systems, i.e.,  $\tau_1 \neq \tau_2$ ; we take  $\tau_1 = 4$  and  $\tau_2 = 3.44$ . As before, for the chaotic oscillation we take  $b_1 = b_2 = 1.65$ . Again, from (2) we have the maximum value of  $f'(y_{\tau_2})$  is equal to 2.114; thus to ensure generalized synchronization we take  $K = 3$ . The real time traces of the driver ( $x(t)$ ) and response ( $y(t)$ ) systems are shown in the Fig. 6 (upper panel), which shows that, unlike complete synchronization, the driver and response are not exactly similar but connected by a functional relation, indicating generalized synchronization. Phase plane plot (middle panel) in the representative  $x(t)$ – $y(t)$  plane shows that the system dynamics do not converge to the straight line but wander around

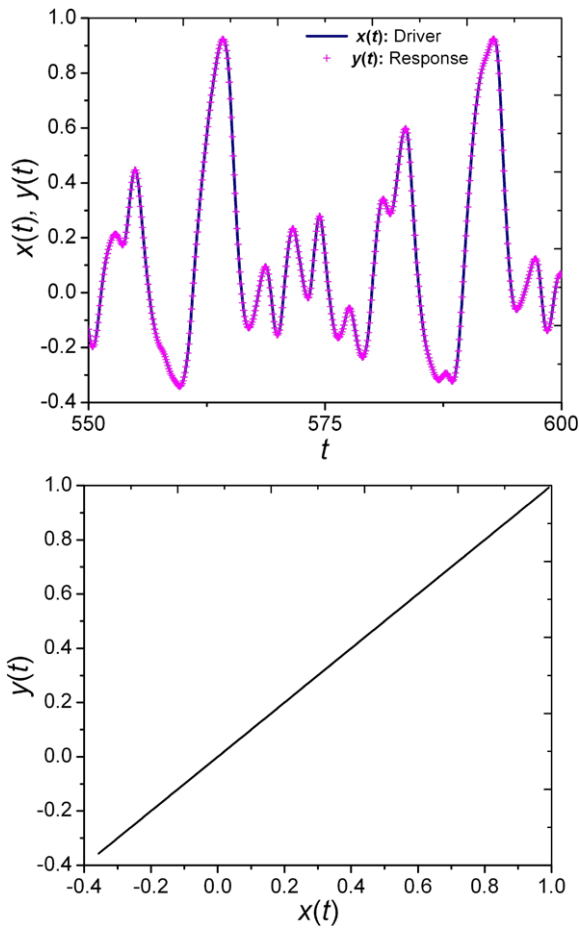


**Fig. 4** Upper panel: Complete synchronization of chaos: Driver  $x(t)$  and Response  $y(t)$  signal ( $K = 3$ ,  $\tau_1 = \tau_2 = 4$ ,  $b_1 = b_2 = 1.65$ ). Lower panel: The corresponding phase plane plot in  $x(t)$ - $y(t)$  plane

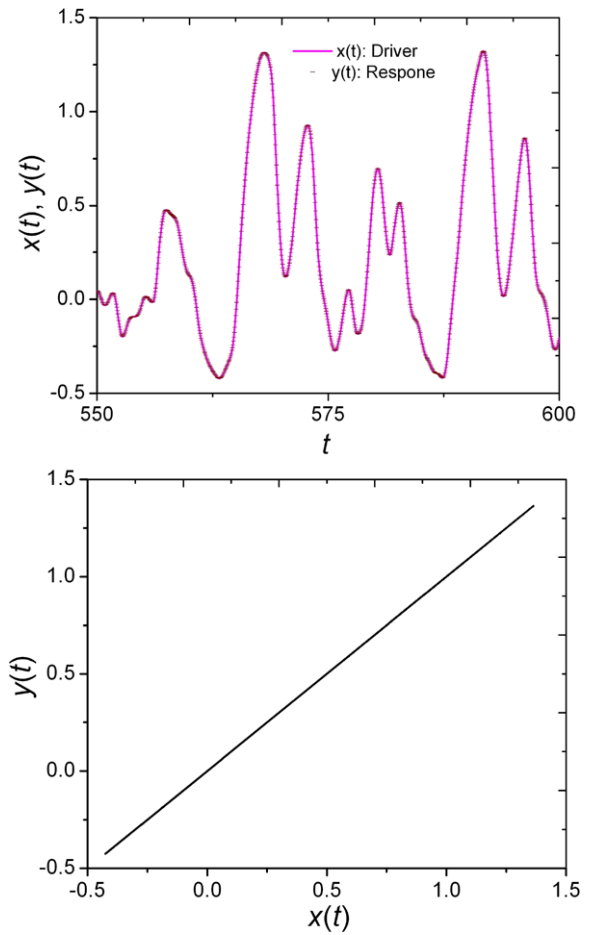


**Fig. 5** Upper panel: Complete synchronization of hyperchaos: Driver  $x(t)$  and Response  $y(t)$  signal ( $K = 3.5$ ,  $\tau_1 = \tau_2 = 4$ ,  $b_1 = b_2 = 2.1$ ). Lower panel: The corresponding phase plane plot in  $x(t)$ - $y(t)$  plane

the straight line that makes a  $45^\circ$  angle to the  $x$ -axis. The real time plot (and also phase plane plot in the inset) of the response  $y(t)$  and the auxiliary variable  $z(t)$  is shown in the lower panel of Fig. 6 that indicates a complete synchronization between them; this, in turn, ensures the occurrence of generalized synchronization between  $x(t)$  and  $y(t)$ .

For the hyperchaotic oscillation, we take  $b_1 = b_2 = 2.1$  and  $K = 3.5$ . Figure 7 shows the real time plots (upper panel) and the phase plane plot (middle panel) of  $x(t)$  and  $y(t)$ , and also plot of  $y(t)$  and  $z(t)$  (lower panel). Since  $y(t) = z(t)$ , thus we can say that  $x(t)$  and  $y(t)$  are in generalized synchronized state in the hyperchaotic region also.

### 6 Electronic circuit realization

To experimentally verify the analytical and numerical findings, we implement the coupled system given by (3a), (3b) in an analog electronic circuit. Figure 8 shows the representative diagram of the experimental circuit. There are two distinct parts, namely, the driver and the response, which are unidirectionally coupled by a resistor  $R_c$  that controls the coupling rate. The nonlinear device (ND) part of each refers to the circuit of Fig. 9; delay block is realized by using active all-pass filters (APF). Let,  $V_1(t)$  be the voltage drop across the capacitor  $C_0$  of the low-pass filter section  $R_0 - C_0$  of the driver and that of the response be  $V_2(t)$ ; thus the following equations represent the time evolu-

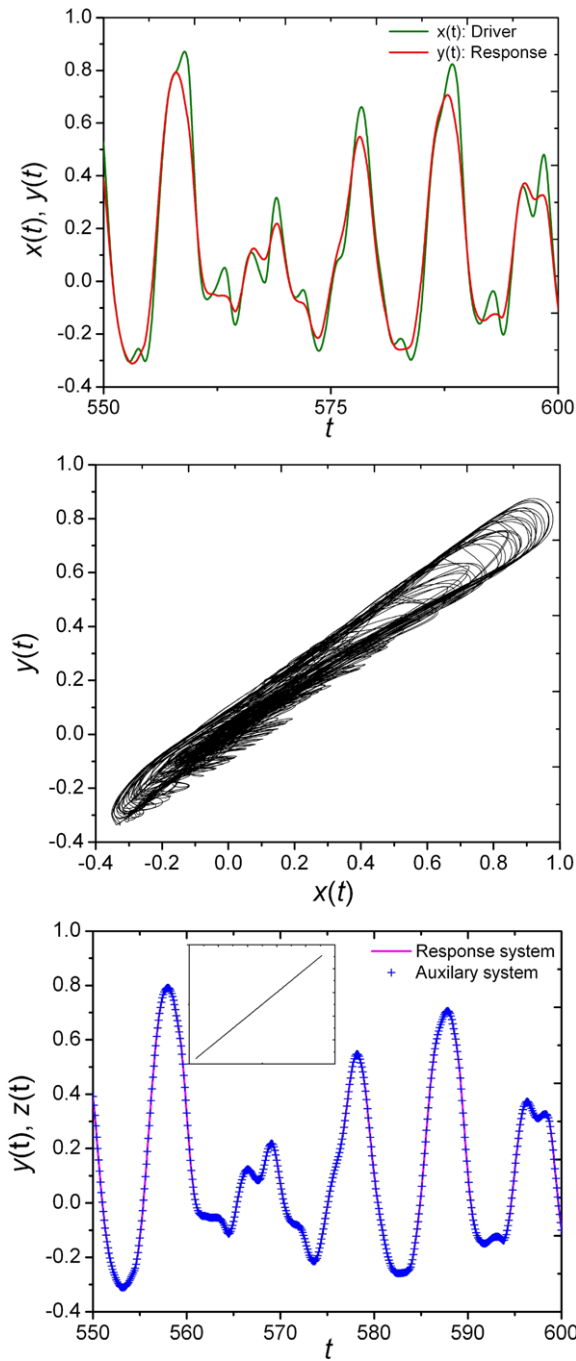


**Fig. 6** Upper panel: Generalized synchronization of chaos: Driver  $x(t)$  and Response  $y(t)$  signal ( $K = 3$ ,  $\tau_1 = 4$ ,  $\tau_2 = 3.44$ ,  $b_1 = b_2 = 1.65$ ). Middle panel: The corresponding phase plane plot in  $x(t)$ - $y(t)$  plane. Lower panel: Complete synchronization between the response  $y(t)$  and the auxiliary variable  $z(t)$ ; inset shows the corresponding phase plane plot in the  $y(t)$ - $z(t)$  plane

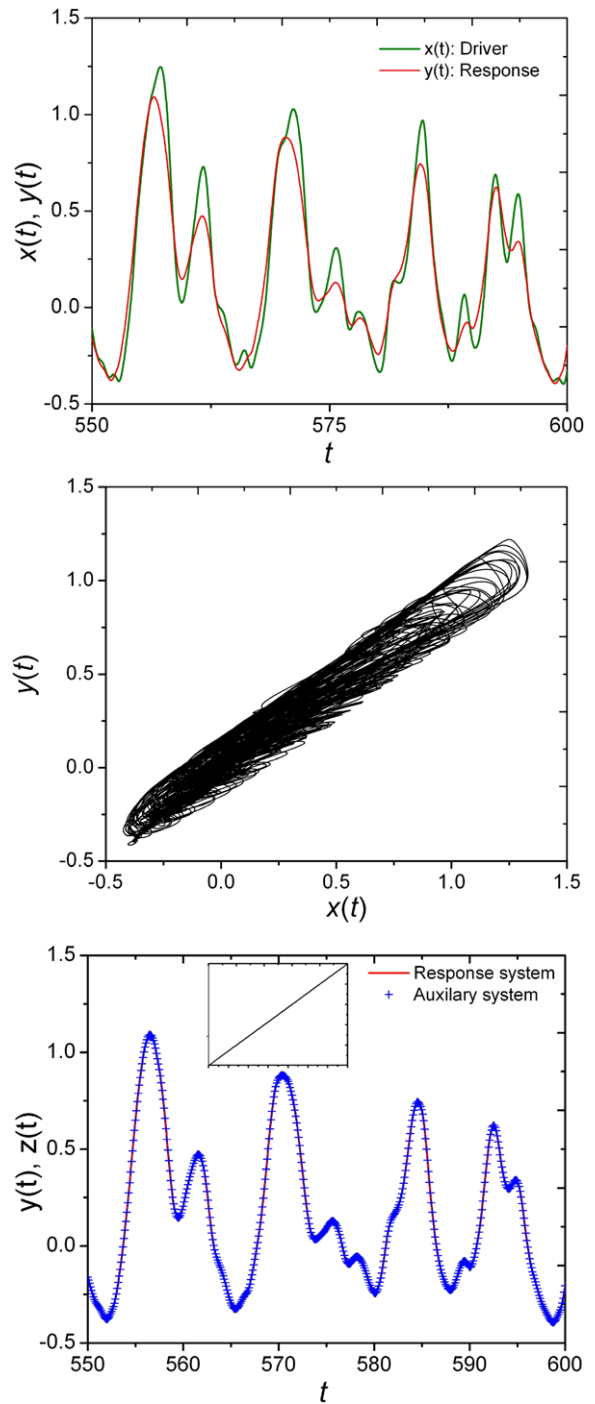


**Fig. 7** Upper panel: Generalized synchronization of hyperchaos: Driver  $x(t)$  and Response  $y(t)$  signal ( $K = 3.5$ ,  $\tau_1 = 4$ ,  $\tau_2 = 3.44$ ,  $b_1 = b_2 = 2.1$ ). Middle panel: The corresponding phase plane plot in  $x(t)$ - $y(t)$  plane. Lower panel: Complete synchronization between the response  $y(t)$  and the auxiliary variable  $z(t)$ ; inset shows the corresponding phase plane plot in the  $y(t)$ - $z(t)$  plane

**Fig. 8** Experimental circuit diagram of the coupled system.  $R_0 = 1\text{ k}\Omega$ ,  $C_0 = 100\text{ nF}$ . Buffers are designed with the unity gain non-inverting operational amplifiers.  $R_c$  determines the coupling rate

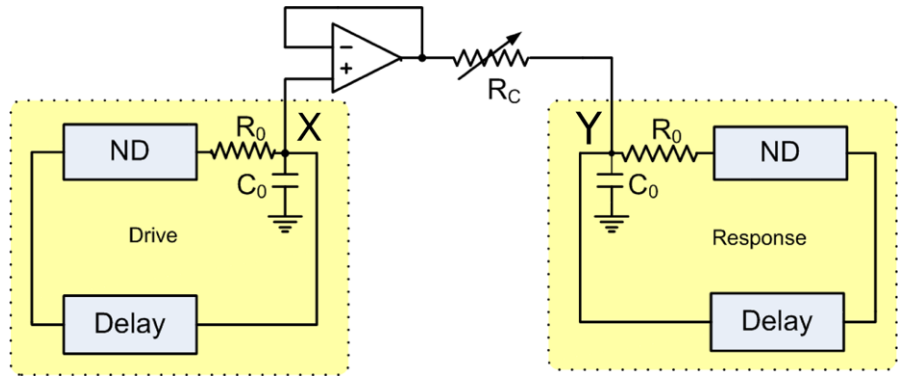
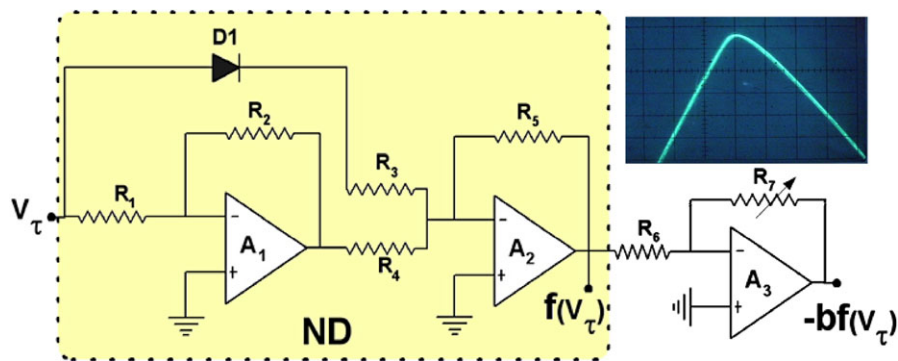


**Fig. 9** Nonlinear Device (ND) along with the amplifying stage (b). A1–A3 are opamps (TL 074), D1 is the diode: 1N4148,  $R_1 = 17.49\text{ k}\Omega$ ,  $R_2 = 12.08\text{ k}\Omega$ ,  $R_3 = 9.78\text{ k}\Omega$ ,  $R_4 = 6.96\text{ k}\Omega$ ,  $R_5 = 10\text{ k}\Omega$ ,  $R_6 = 1\text{ k}\Omega$ . Inset shows the experimental oscilloscope trace of the nonlinearity produced by the ND



tion of the circuit:

$$R_0 C_0 \frac{dV_1(t)}{dt} = -V_1(t) - b_1 f(V_1(t - T_{D1})), \quad (13)$$

$$R_0 C_0 \frac{dV_2(t)}{dt} = -V_2(t) - b_2 f(V_2(t - T_{D2})) + K(V_1(t) - V_2(t)). \quad (14)$$

Here,  $b_1, b_2 = \frac{R_7}{R_6}$  is the gain of the amplifier A3 (Fig. 9), and  $K = 1/R_c$  is the coupling rate.  $f(V(t - T_{D_i})) \equiv f(V_{\tau_i}), i = 1, 2$ , is the nonlinear function representing the output of the Nonlinear Device (ND) of Fig. 9, in terms of the input voltage  $V_{\tau_i}$ .  $T_{D_i}$  is the time delay produced by the delay block.

In [1], we have reported that the nonlinearity of Fig. 9 has the following form:

$$f(V(t - T_{D_i})) = -\frac{R_5}{R_3} 0.5[|V(t - T_{D_i})| + V(t - T_{D_i})] + \frac{R_5}{R_4} \beta V_{\text{sat}} \tanh\left(w \frac{R_2}{R_1} \frac{V(t - T_{D_i})}{V_{\text{sat}}}\right). \quad (15)$$

The variable delay element is realized by a first-order all-pass filter (APF) (Fig. 10) [43]. The APF has the following transfer function:

$$T(s) = -a_1 \frac{s - \omega_0}{s + \omega_0} \quad (16)$$

with flat gain  $a_1 = 1$  (determined by  $R_8$  and  $R_9$ ), and  $\omega_0 = 1/CR$  is the frequency at which the phase shift is  $\pi/2$ . Since it has an almost linear phase response, thus each APF block contributes a delay of  $T_D \approx RC$ . So  $j$  blocks produce a delay of  $T_D = jRC$  ( $j = 1, 2, \dots$ ). By simply changing the resistance  $R$ , one can vary the amount of delay; thus one can control the resolution of the delay line.

Let us define the following dimensionless variables and parameters:  $t = \frac{t}{R_0 C_0}$ ,  $\tau_i = \frac{T_{D_i}}{R_0 C_0}$ ,  $x = \frac{V_1(t)}{V_{\text{sat}}}$ ,  $x(t - \tau_1) = \frac{V_1(t - T_{D1})}{V_{\text{sat}}}$ ,  $y = \frac{V_2(t)}{V_{\text{sat}}}$ ,  $y(t - \tau_2) = \frac{V_2(t - T_{D2})}{V_{\text{sat}}}$ ,  $\frac{R_5}{R_3} = n_1$ ,  $\beta \frac{R_5}{R_4} = m_1$ ,  $w \frac{R_2}{R_1} = l_1$ ,  $b_i = \frac{R_7}{R_6}$ , and  $K = \frac{1}{R_c}$ , where  $i = 1, 2$ . Now, (13), (14), and (15) can be reduced to the following dimensionless, coupled, first-order, nonlinear delay differential equations:

$$\frac{dx}{dt} = -x(t) - b_1 f(x(t - \tau_1)), \quad (17)$$



$$\frac{dy}{dt} = -y(t) - b_2 f(y(t - \tau_2)) + K(x - y). \quad (18)$$

where

$$\begin{aligned} f(u(t - \tau_i)) &\equiv f(u_{\tau_i}) \\ &= -n_1 0.5(|u_{\tau_i}| + u_{\tau_i}) \\ &\quad + m_1 \tanh(l_1 u_{\tau_i}), \end{aligned} \quad (19)$$

where  $u \equiv x, y$ .

It is worth noting that (17) and (18) (along with (19)) are equivalent to (3a) and (3b) (along with (2)) with  $a = 1$ , and appropriate choices of  $n_1, m_1$  and  $l_1$ .

### 7 Experimental results

The coupled system is designed on hardware level on a bread board using IC TL074 opamps (JFET quad opamps) with a  $\pm 15$  volt power supply. Capacitors and resistors have 5 % tolerance. The resistance values used in the circuits for both the driver and response are:  $R_1 = 17.49 \text{ k}\Omega, R_2 = 12.08 \text{ k}\Omega, R_3 = 9.78 \text{ k}\Omega, R_4 = 6.96 \text{ k}\Omega, R_5 = 10 \text{ k}\Omega, R_6 = 1 \text{ k}\Omega$ . For the low-pass section we used  $R_0 = 1 \text{ k}\Omega$  and  $C_0 = 100 \text{ nF}$ . The nonlinearity produced by the nonlinear device part of all the systems are kept similar in nature and is shown in Fig. 9 (inset). The delay is implemented by the use of identical active all-pass filter stages shown in Fig. 10, with specifications  $R_8 = R_9 = 2.2 \text{ k}\Omega, C = 10 \text{ nF}$  and a variable resistance  $R$ . Here our main concern is to study the synchronization phenomena by varying the system delays of the constituent systems keeping the other system design-parameters same for the two systems.

#### 7.1 Uncoupled condition

In the uncoupled condition, the isolated systems show chaos and hyperchaos when we vary the parameter controlling the gain of the circuit, viz., the resistance  $R_7$ . The individual systems show chaos for  $R_7 \geq 2.52 \text{ k}\Omega$  and hyperchaos for  $R_7 \geq 2.66 \text{ k}\Omega$ . Figure 11 shows the oscilloscope traces of chaos and hyperchaos of the driver and response for  $R_7 = 2.60 \text{ k}\Omega$  and  $R_7 = 2.71 \text{ k}\Omega$ , respectively. The first two traces on the left column show the chaotic attractors of uncoupled driver and response, respectively. The third trace in the left

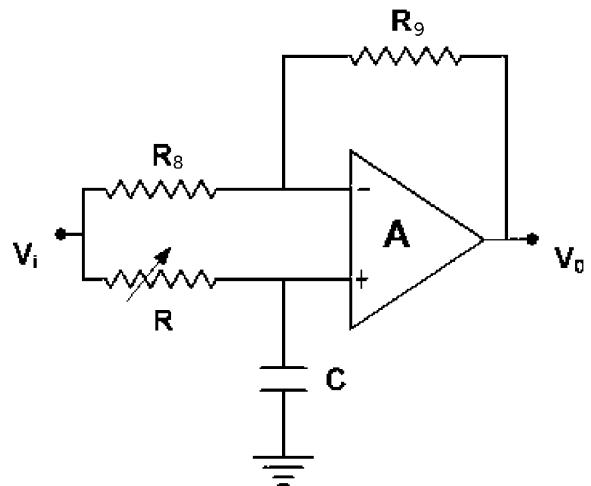


**Fig. 10** Active first-order all-pass filter.  $R_8 = R_9 = 2.2 \text{ k}\Omega, C = 10 \text{ nF}$

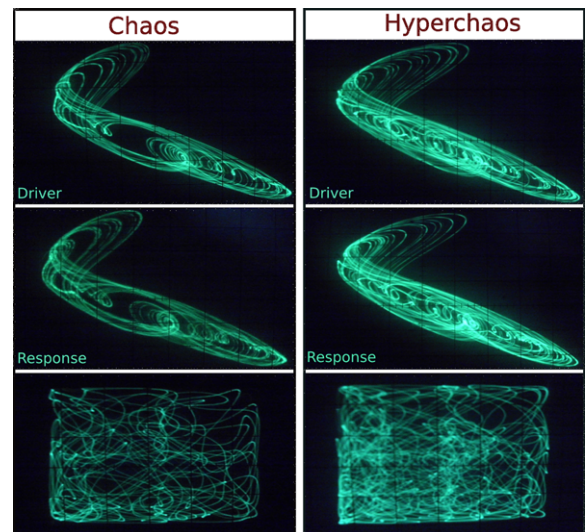


**Fig. 11** The individual attractors of the uncoupled driver (in  $V_1(t) - V_1(t - T_D)$  space) and the response (in  $V_2(t) - V_2(t - T_D)$  space) in chaotic (left column) and hyperchaotic regime (right column). Lower panel shows the corresponding experimental phase plane plots in the  $V_1(t) - V_2(t)$  space. Oscilloscope scale divisions: x-axis:  $0.2 \text{ v/div}$ , y-axis:  $0.2 \text{ v/div}$

column represents the experimental phase plane plot in the  $V_1(t) - V_2(t)$  space, which indicates that there is no correlation between the constituent systems indicating an unsynchronized response of the driver and response. This observations are repeated for the hyperchaotic oscillation also and depicted in the right column of the same figure.

## 7.2 Coupled system in the chaotic regime

For chaotic oscillation we choose  $R_7 = 2.60 \text{ k}\Omega$ . In the chaotic mode, on varying the system delays, we observe the following synchronization scenario.

(i) We keep the system delays equal,  $\tau_1 = \tau_2 = 4$ . To implement this delay we use four similar stages of APF with  $R = 10 \text{ k}\Omega$ . We observe that the complete synchronization (CS) is obtained when the coupling resistor is made  $R_c \leq 59 \Omega$ . Figure 12(a1) shows the experimental time series of the driver and the response recorded by a digital storage oscilloscope (Tektronix, TDS2002B, 60 MHz, 1 GS/s); Fig. 12(a2) shows the corresponding phase plane plot in the  $V_1(t) - V_2(t)$  space ( $R_c \approx 50 \Omega$ ). From the time series it is clear that both the driver and the response systems have the same waveform, and the phase space diagram is a straight line inclined at  $45^\circ$  with each axes, which strongly support the occurrence of complete synchronization.

(ii) Next, we consider the case for  $\tau_1 \neq \tau_2$ . In our experiment we use  $\tau_1 = 4$  and  $\tau_2 = 3.44$ . We observe the generalized synchronization (GS) when the coupling resistor becomes  $R_c \leq 260 \Omega$ . Figure 12(b1) shows the experimental time series of the GS ( $R_c \approx 250 \Omega$ ), and Fig. 12(b2) the corresponding synchronization manifold in the  $V_1(t) - V_2(t)$  space. The time series plot and the phase plane plot clearly show that the response tries to imitate the driver, which is the characteristic of generalized synchronization.

For the experimental confirmation of generalized synchronization, we design an auxiliary system which is identical to the response system; the response and the auxiliary systems are coupled with the driver by a unidirectional, linear, dissipative coupling. In support of the above mentioned observations, it is observed that when ever the driver and the response are in generalized synchronized mode, the response and the auxiliary systems show a complete synchronization between them. Figure 12(c1) shows the experimental time series of the response and the auxiliary system, and Fig. 12(c2) represents the corresponding phase plane plot; both the observations ensure the complete synchronization of the response and the auxiliary system that, in turn, ensures the generalized synchronization between the driver and the response.

## 7.3 Coupled system in the hyperchaotic regime

We choose  $R_7 = 2.71 \text{ k}\Omega$  for the hyperchaotic oscillation. In the hyperchaotic regime also we observe two

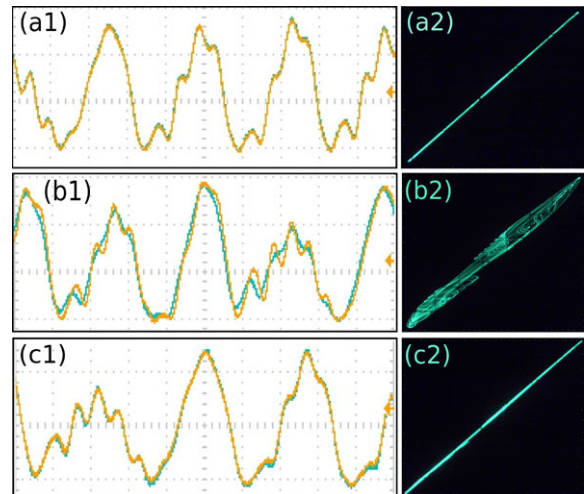


**Fig. 12** Experimental time series plot of the driver  $V_1(t)$  (yellow) and the response  $V_2(t)$  (cyan) in the Chaotic Regime: **(a1)** complete synchronization ( $\tau_1 = \tau_2 = 4$ ), **(b1)** generalized synchronization ( $\tau_1 = 4$ ,  $\tau_2 = 3.44$ ) **(c1)** Complete synchronization between the response and the auxiliary system. The corresponding phase plane plots are shown in **(a2)** CS, **(b2)** GS, and **(c2)** CS of response and auxiliary system. For **(a1)**, **(b1)**, and **(c1)**: x-axis:  $50 \mu\text{s/div}$ , y-axis:  $0.37 \text{ v/div}$ . For **(a2)**, **(b2)**, and **(c2)**: x-axis:  $0.2 \text{ v/div}$ , y-axis:  $0.2 \text{ v/div}$  (Color figure online)

types of synchronization, namely, complete and generalized synchronization.

(i) To observe CS, we equate the system delays, fixing  $\tau_1 = \tau_2 = 4$ . We observe CS for  $R_c \leq 56 \Omega$ . Figure 13(a1) shows the experimental time series of the driver and the response ( $R_c \approx 50 \Omega$ ), Fig. 13(a2) shows the synchronization manifold, supporting the properties of complete synchronization.

(ii) The GS is achieved for the unequal system delays  $\tau_1 = 4$  and  $\tau_2 = 3.44$ , and  $R_c \leq 242 \Omega$ . Figure 13(b1), (b2) shows the time series of the driver and the response ( $R_c \approx 230 \Omega$ ), and synchronization manifold, respectively, which indicate generalized synchronization. Figure 13(c1), (c2) represents the experimental time series and the phase plane plot of the response and the auxiliary system indicating complete synchronization between them, which, in turn, ensures the generalized synchronization between the hyperchaotic driver and response.

## 8 Conclusion

In this paper we have reported different synchronization scenario of a coupled first-order, time-delayed

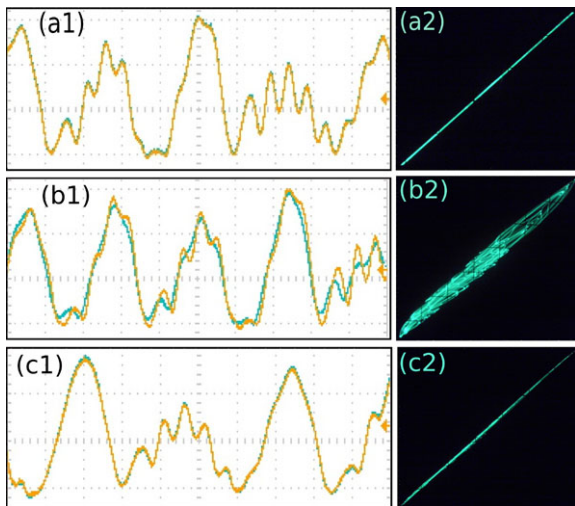


**Fig. 13** Experimental time series plot of the driver  $V_1(t)$  (yellow) and the response  $V_2(t)$  (cyan) in the *Hyperchaotic Regime*: (a1) complete synchronization ( $\tau_1 = \tau_2 = 4$ ), (b1) generalized synchronization ( $\tau_1 = 4$ ,  $\tau_2 = 3.44$ ), (c1) Complete synchronization between the response and the auxiliary system. The corresponding phase plane plots are shown in (a2) CS, (b2) GS, and (c2) CS of response and auxiliary system. Scale divisions are same as Fig. 12 (Color figure online)

chaotic (hyperchaotic) system. The system we have chosen is a first-order, nonlinear time-delayed system recently proposed by Banerjee et al. [1], which possesses a closed form mathematical function for the nonlinearity and shows hyperchaos even at a moderate or small time delay. We have considered a unidirectional, linear, dissipative coupling scheme between the driver and the response. It has been shown that keeping all other parameters the same if we make the system delays of both the systems similar, then beyond a certain coupling strength complete synchronization occurs; on the other hand, unequal system delays result in generalized synchronization. The stability conditions for both synchronization scenarios have been derived analytically using Krasovskii–Lyapunov theory. Numerical simulations have been carried out to corroborate the analytical results. Further, we implement an experimental setup at the electronic circuit level to demonstrate the synchronization scenario. We design an auxiliary system to *experimentally* confirm the occurrence of generalized synchronization. Experimental real-time observations are in full agreement with the analytical and numerical results.

As the system under study is simple and well characterized, and also is capable of producing hyperchaotic oscillations for a small time delay, thus, apart

from the academic merits, all the observations reported in this paper regarding the synchronization scenario may be helpful towards the implementation of a chaos and hyperchaos-based communication scheme. Also, synchronizations of the present system with other coupling schemes can be explored and deserve further study.

**Acknowledgements** One of the authors (D.B.) thankfully acknowledges the financial support provided by the University of Burdwan.

## References

- Banerjee, T., Biswas, D., Sarkar, B.C.: Design and analysis of a first order time-delayed chaotic system. *Nonlinear Dyn.* (2012). doi:10.1007/s11071-012-0490-3. Published online 12 June 2012
- Pecora, L.M., Carroll, T.L.: Synchronization in chaotic systems. *Phys. Rev. Lett.* **64**, 821–824 (1990)
- Rulkov, N.F., Sushchik, M.M., Tsimring, L.S., Abarbanel, H.D.I.: Generalized synchronization of chaos in directionally coupled chaotic systems. *Phys. Rev. E* **51**, 980–994 (1995)
- Abarbanel, H.D.I., Rulkov, N.F., Sushchik, M.M.: Generalized synchronization of chaos: the auxiliary system approach. *Phys. Rev. E* **53**, 4528–4535 (1996)
- Cai, N., Li, W., Jing, Y.: Finite-time generalized synchronization of chaotic systems with different order. *Nonlinear Dyn.* **64**, 385–393 (2011)
- Rosenblum, M.G., Pikovsky, A.S., Kurths, J.: Phase synchronization of chaotic oscillators. *Phys. Rev. Lett.* **76**, 1804–1807 (1996)
- Rosenblum, M.G., Pikovsky, A.S., Kurths, J.: From phase to lag synchronization in coupled chaotic oscillators. *Phys. Rev. Lett.* **78**, 4193–4197 (1997)
- Miao, Q., Tang, Y., Lu, S., Fang, J.: Lag synchronization of a class of chaotic systems with unknown parameters. *Nonlinear Dyn.* **57**, 107–112 (2009)
- Voss, H.U.: Anticipating chaotic synchronization. *Phys. Rev. E* **61**, 5115–5119 (2002)
- Amritkar, R.E., Gupte, N.: Synchronization of chaotic orbits: the effect of a finite time step. *Phys. Rev. E* **47**, 3889–3895 (1993)
- Stojanovski, T., Kocarev, L., Parlitz, U.: Driving and synchronizing by chaotic impulses. *Phys. Rev. E* **54**, 2128–2131 (1996)
- Pecora, L.M., Carroll, T.L., Johnson, G.A., Mar, D.J.: Fundamentals of synchronization in chaotic systems, concepts, and applications. *Chaos* **7**, 4 (1997)
- Boccaletti, S., Kurths, J., Osipov, G., Valladares, D.L., Zhou, C.S.: The synchronization of chaotic systems. *Phys. Rep.* **366**, 1–101 (2002)
- Peng, J.H., Ding, E.J., Ding, M., Yang, W.: Synchronizing hyperchaos with a scalar transmitted signal. *Phys. Rev. Lett.* **76**, 904–907 (1996)

15. Frasca, M., Buscarino, A., Rizzo, A., Fortuna, L., Boccaletti, S.: Synchronization of moving chaotic agents. *Phys. Rev. Lett.* **100**, 044102 (2008)
16. Mackey, M.C., Glass, L.: Oscillation and chaos in physiological control system. *Science* **197**, 287–289 (1977)
17. Ikeda, K., Daido, H., Akimoto, O.: Optical turbulence: chaotic behavior of transmitted light from a ring cavity. *Phys. Rev. Lett.* **45**, 709–712 (1980)
18. Wei, J., Yu, C.: Stability and bifurcation analysis in the cross-coupled laser model with delay. *Nonlinear Dyn.* **66**, 29–38 (2011)
19. Yongzhen, P., Shuping, L., Changguo, L.: Effect of delay on a predator–prey model with parasitic infection. *Nonlinear Dyn.* **63**, 311–321 (2011)
20. Pei, L., Wang, Q., Shi, H.: Bifurcation dynamics of the modified physiological model of artificial pancreas with insulin secretion delay. *Nonlinear Dyn.* **63**, 417–427 (2011)
21. Boutle, I., Taylor, R.H.S., Romer, R.A.: El Niño and the delayed action oscillator. *Am. J. Phys.* **75**, 15–24 (2007)
22. Liao, X., Guo, S., Li, C.: Stability and bifurcation analysis in tri-neuron model with time delay. *Nonlinear Dyn.* **49**, 319–345 (2007)
23. Le, L.B., Konishi, K., Hara, N.: Design and experimental verification of multiple delay feedback control for time-delay nonlinear oscillators. *Nonlinear Dyn.* **67**, 1407–1418 (2012)
24. Kwon, O.M., Park, J.H., Lee, S.M.: Secure communication based on chaotic synchronization via interval time-varying delay feedback control. *Nonlinear Dyn.* **63**, 239–252 (2011)
25. Ji, J.C., Hansen, C.H., Li, X.: Effect of external excitations on a nonlinear system with time delay. *Nonlinear Dyn.* **41**, 385–402 (2005)
26. Ramana Reddy, D.V., Sen, A., Johnston, G.L.: Sen:time delay induced death in coupled limit cycle oscillators. *Phys. Rev. Lett.* **80**, 5109–5112 (1998)
27. Pyragas, K.: Synchronization of coupled time-delay systems: analytical estimation. *Phys. Rev. E, Stat. Nonlinear Soft Matter Phys.* **58**, 3067–3071 (1998)
28. Zhan, M., Wang, X., Gong, X., Wei, G.W., Lai, C.H.: Complete synchronization and generalized synchronization of one-way coupled time-delay systems. *Phys. Rev. E* **68**, 036208 (2003)
29. Sahaverdiev, E.M., Shore, K.A.: Generalized synchronization in time-delayed systems. *Phys. Rev. E, Stat. Nonlinear Soft Matter Phys.* **71**, 016201 (2005)
30. Senthilkumar, D.V., Lakshmanan, M.: Transition from anticipatory to lag synchronization via complete synchronization in time-delay systems. *Phys. Rev. E* **71**, 016211 (2005)
31. Srinivasan, K., Senthilkumar, D.V., Murali, K., Lakshmanan, M., Kurths, J.: Synchronization transitions in coupled time-delay electronic circuits with a threshold nonlinearity. *Chaos* **21**, 023119 (2011)
32. Nayfeh, A.H., Balachandran, B.: *Applied Nonlinear Dynamics: Analytical, Computational, and Experimental Methods*. Wiley, New York (1995)
33. Perez, G., Cerdeira, H.: Extracting messages masked by chaos. *Phys. Rev. Lett.* **74**, 1970–1973 (1995)
34. Kye, W.-H., Choi, M., Kurdoglyan, M.S., Kim, C.-M., Park, Y.-J.: Synchronization of chaotic oscillators due to common delay time modulation. *Phys. Rev. E* **70**, 046211 (2004)
35. Namajunas, A., Pyragas, K., Tamaševičius, A.: An electronic analog of the Mackey–Glass system. *Phys. Lett. A* **201**, 42–46 (1995)
36. Lu, H., He, Y., He, Z.: A chaos-generator: analysis of complex dynamics of a cell equation in delayed cellular neural networks. *IEEE Trans. Circuits Syst. I, Fundam. Theory Appl.* **45**, 178–181 (1998)
37. Mykolaitis, G., Tamaševičius, A., Čenys, A., Bumeliene, S., Anagnostopoulos, A.N., Kalkan, N.: Very high and ultrahigh frequency hyperchaotic oscillators with delay line. *Chaos Solitons Fractals* **17**, 343 (2003)
38. Tamaševičius, A., Pyragas, T., Meskauskas, M.: Two scroll attractor in a delay dynamical system. *Int. J. Bifurc. Chaos Appl. Sci. Eng.* **17**(10), 3455–3460 (2007)
39. Buscarino, A., Fortuna, L., Frasca, M., Sciuto, G.: Design of time-delay chaotic electronic circuits. *IEEE Trans. Circuits Syst. I, Fundam. Theory Appl.* **58**, 1888–1896 (2011)
40. Pham, V.-T., Fortuna, L., Frasca, M.: Implementation of chaotic circuits with a digital time-delay block. *Nonlinear Dyn.* **67**, 345–355 (2012)
41. Leonov, G.A., Kuznetsov, N.V.: Time-varying linearization and the Perron effects. *Int. J. Bifurc. Chaos Appl. Sci. Eng.* **17**, 1079–1107 (2007)
42. Krasovskii, N.N.: *Stability of Motion*. Stanford University Press, Stanford (1963)
43. Sedra, A.S., Smith, K.C.: *Microelectronic Circuits*. Oxford Univ. Press, London (2003)